

Electroabsorption Studies of Intervalence Charge Transfer in $(\text{NC})_5\text{FeCNOs}(\text{NH}_3)_5^-$: Experimental Assessment of Charge-Transfer Distance, Solvent Reorganization, and Electronic Coupling Parameters

Laba Karki, Hong Peter Lu,[†] and Joseph T. Hupp*

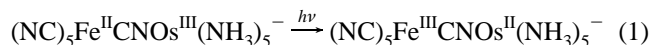
Department of Chemistry, Northwestern University, Evanston, Illinois 60208

Received: May 10, 1996; In Final Form: July 17, 1996[Ⓢ]

Electroabsorption studies of $(\text{NC})_5\text{FeCNOs}(\text{NH}_3)_5^-$ show that light-induced metal-to-metal charge transfer is accompanied by a dipole moment change of -12.5 ± 1.5 D along the charge-transfer axis. This change corresponds to an effective one-electron transfer distance of 2.5 ± 0.3 Å, i.e., less than half the geometric distance from iron to osmium. The charge-transfer distance revision has profound effects upon estimates for solvent reorganization and nonadiabatic electronic coupling energies. The distance revision decreases the former from 7000 to 2200 cm^{-1} and increases the latter from 1260 to 2600 cm^{-1} . Reliable estimates for both, of course, are required in order to understand light-induced electron-transfer kinetics.

Introduction

Electroabsorption or electronic Stark effect measurements offer a direct means for assessing effective one-electron-transfer distances for optical transitions, d .^{1–3} Besides providing basic chemical insight, the distance assessments are crucial for the accurate evaluation of solvent reorganization energies and initial-state/final-state electronic coupling matrix elements.^{4–7} Here we describe the application of electroabsorption spectroscopy to the intervalence charge transfer reaction shown in eq 1. This



system is one member of a class of mixed-valence systems that has been extensively investigated with regard to both thermal and optical electron-transfer (ET) energetics, kinetics and dynamics.^{8–12} As discussed below, Stark measurements provide important new information that is essential for the accurate interpretation of many existing experiments. To the best of our knowledge, previous applications of Stark effect spectroscopy to mixed-valence systems have been limited to $(\text{NH}_3)_5\text{Ru}$ –pyrazine– $\text{Ru}(\text{NH}_3)_5^{5+}$ (a valence-delocalized system) and its 4,4'-bipyridine-bridged analogue.²

Experimental Section

Stark measurements were made at 77 K in a 1:1 (v:v) ethylene glycol:water glass by using a retrofitted Cary 14 spectrophotometer featuring OLIS control software. The pathlength of the cell (indium–tin oxide coated quartz plates; Kapton tape spacers) was ca. 100 μm (measured interferometrically in the near-IR region with an empty cell). The maximum field strength (rms) was 3.5×10^7 V/m.¹³ The second-order Stark signal ($i_{2\omega}$) was detected with a photomultiplier tube (R928) with five dynode stages, and a digital lock-in amplifier (Stanford Research Systems, Model SR 850) at twice the field modulation frequency, ω (typically 250 Hz).

Changes in dipole moment and polarizability were extracted from electroabsorption spectra via a least-squares fitting procedure that will be fully described elsewhere.¹⁶ Briefly, however, after correction for finite bandpass effects and lock-

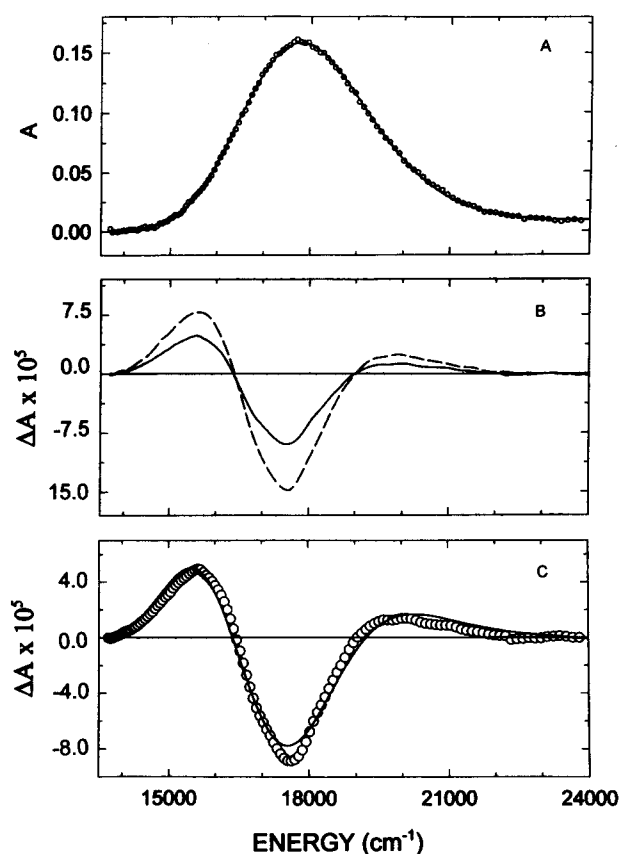


Figure 1. (A) Experimental absorption spectrum for $(\text{NC})_5\text{Fe}^{\text{II}}\text{CNOs}^{\text{III}}(\text{NH}_3)_5^-$ at 77 K (circles) and Gaussian fit (line). (B) Stark spectra at $\chi = 90^\circ$ (solid line) and 55° (dashed line). (C) Least-squares fit (solid line) of 90° Stark spectrum (circles) to eq 2.

in amplifier time constant effects, electroabsorption spectra obtained at two angles were fit to a linear combination of zero, first, and second derivatives of a Gaussian representation of the energy weighted absorption spectrum.

Results and Discussion

Figure 1 (top panel) shows an absorption spectrum for $(\text{NC})_5\text{Fe}^{\text{II}}\text{CNOs}^{\text{III}}(\text{NH}_3)_5^-$ (1) at 77 K, where the absorption

[†] Current address: Pacific Northwest Laboratory, Richland, WA.

[Ⓢ] Abstract published in *Advance ACS Abstracts*, September 15, 1996.

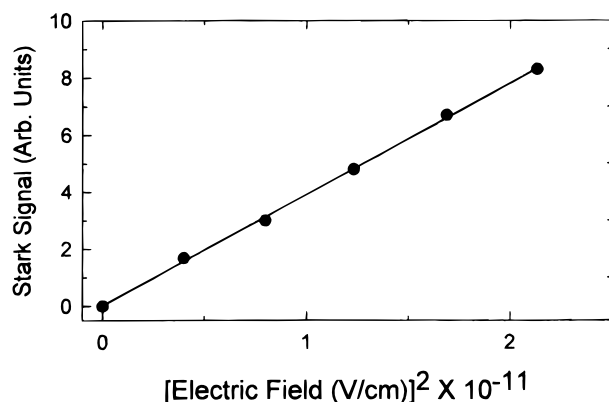


Figure 2. Field dependence of Stark signal for $(\text{NC})_5\text{FeCNOs}(\text{NH}_3)_5^-$.

maximum is blue-shifted by 1400 cm^{-1} from its value at room temperature. Figure 1b shows the experimental Stark response (i.e., field on–field off) at $\chi = 55^\circ$ and 90° . (χ is the angle between the applied electric field, \mathbf{F} , and the electric polarization vector of the incident light beam.) Note the approximate “second-derivative” shape for the electroabsorption spectrum. Additional experiments (Figure 2) established that the Stark signals vary, as expected, with the field strength squared (see eq 2).

To interpret the experiment, we assumed (following Liptay¹⁴) that the external electric field could alter the molar extinction coefficient, ϵ , and therefore the absorbance, A , by changing (a) the transition moment, \mathbf{P}_{12} , (b) the energy difference, $h\Delta\nu_{12}$, between the final state (2) and initial state (1), and/or (c) the absorption line shape. (Subscript numbers denote adiabatic states; subscript letters denote fully localized, or diabatic, states.) If the external field is uniform, the sample is isotropic and the molecular dipoles have frozen orientations, then the Stark absorption signal ($\Delta A(\nu)$) can be quantitatively represented as the following linear combination of zero, first, and second derivatives of the absorption band, $A(\nu)$:^{1,2,14}

$$\Delta A(\nu) = \left\{ A_x A(\nu) + \frac{B_x}{15hc} \frac{v d[A(\nu)/v]}{dv} + \frac{C_x}{30h^2 c^2} \frac{v d^2[A(\nu)/v]}{dv^2} \right\} \mathbf{F}_{\text{int}}^2 \quad (2)$$

where \mathbf{F}_{int} is the internal electric field (i.e., the field actually experienced by the chromophore),¹⁵ ν is the frequency of the absorbed light, h is Planck’s constant, and c is the speed of light. The coefficients A_x , B_x , and C_x have been described in detail previously.^{1,2,14} Briefly, however, A_x provides information about the transition moment polarizability and hyperpolarizability, B_x describes the difference in polarizability ($\Delta\alpha_{12}$) between the final and initial electronic states along the charge-transfer axis, and C_x describes the difference in dipole moment ($\Delta\mu_{12}$) between the states (where we have employed a sign convention that makes the dipole moments positive quantities).

Figure 1c shows the best fit to the Stark signal at 90° , using the three modeling parameters from eq 2.¹⁶ From the fit (and an additional fit at 55°), $\Delta\mu_{12}$ is $-12.5 \pm 1.5 \text{ D}$, the trace of the polarizability change, $\text{Tr } \Delta\alpha_{12}$ is $-170 \pm 50 \text{ \AA}^3$, and the angle, ξ , between the vectors describing the transition dipole moment and the change in dipole moment is $2 \pm 3^\circ$. A near-zero value for ξ would be expected if the vectors were collinear along the metal–bridge–metal axis. The zeroth-derivative contribution to the Stark signal was found to be negligible, implying very little change in \mathbf{P}_{12} .

The measured change in dipole moment can be related directly to the effective charge-transfer distance, R_{12} , via eq 3^{2–4,6}

$$\Delta\mu_{12} = eR_{12} \quad (3)$$

where e is the unit electronic charge. On this basis, R_{12} is $2.5 \pm 0.3 \text{ \AA}$, i.e., less than half the estimated metal–metal separation distance of 5.3 \AA ! Reimers and Hush⁴ as well as Shin et al.³ have identified several factors that can contribute to differences between “geometric” and actual charge-transfer distances. One is partial electronic delocalization, a factor that could be significant here in view of the high oscillator strength for transition 1 and the general efficacy of cyanide as a donor–acceptor bridge. The magnitude of the delocalization effect can be estimated by comparing R_{12} to the diabatic charge-transfer distance, R_{ab} , available from eqs 4 and 5:^{3,6}

$$\Delta\mu_{\text{ab}} = eR_{\text{ab}} = [(\Delta\mu_{12})^2 + 4\mathbf{P}_{12}^2]^{1/2} \quad (4)$$

$$\mathbf{P}_{12} = 2.06 \times 10^{-2} (\epsilon_{\text{max}} \Delta\nu_{1/2} / \nu_{\text{max}} b)^{1/2} \quad (5)$$

For transition 1 at 77 K , ϵ_{max} is $3600 \text{ cm}^{-1} \text{ M}^{-1}$, the absorption bandwidth, $\Delta\nu_{1/2}$, is 3400 cm^{-1} , and the absorption band maximum, ν_{max} , is $17\,800 \text{ cm}^{-1}$. The degeneracy term, b , is 2 and accounts for the possibility of optical ET from either of two equivalent donor orbitals (i.e., $d_{xz}(\text{Fe})$ or $d_{yz}(\text{Fe})$, where the third potential donor orbital, $d_{xy}(\text{Fe})$, is orthogonal to the charge-transfer axis (z axis) and therefore unable to participate). From the equations, \mathbf{P}_{12} is $0.39 e \text{ \AA}$ (2.0 D) and R_{ab} is 2.6 \AA , i.e., only marginally greater than the adiabatic distance. The remaining differences between observed and geometric distances are likely associated with a combination of ligand permanent dipole effects and excited-state repolarization effects,^{3,4} where the effects can be separated only with significant computational effort.

The observation of an unusually short adiabatic charge-transfer distance has significant implications for the evaluation of ambient temperature solvent reorganizational effects.¹⁷ If these effects are estimated classically via an ellipsoidal cavity model, the value of the solvent reorganization energy, λ_s , is strongly dependent on the effective charge-transfer distance or “dipole switch” size. For $R = 5.3 \text{ \AA}$, the model of Brunschwig et al.¹⁸ yields 7000 cm^{-1} for λ_s , a number clearly inconsistent with the observed lineshape, once vibrational effects^{10a} are considered. For $R = 2.5 \text{ \AA}$,¹⁷ on the other hand, λ_s is only 2200 cm^{-1} . The large revision provided by the electroabsorption experiment obviously has substantial implications in terms of the energetics and presumably, kinetics, of the back-ET (thermal ET) reaction associated with eq 1.

Finally, the availability of the diabatic charge-transfer distance makes possible the assessment of the electronic coupling matrix element, H_{ab} .^{5,6}

$$H_{\text{ab}} = \mathbf{P}_{12} \nu_{\text{max}} / \Delta\mu_{\text{ab}} \quad (6)$$

From eq 6, with $\Delta\mu_{\text{ab}} = 13 \text{ D}$, H_{ab} is 2600 cm^{-1} . On the other hand, if the charge-transfer distance were naively assumed to be the metal–metal separation distance, $\Delta\mu_{\text{ab}}$ would be 26.5 D and H_{ab} would equal just 1260 cm^{-1} . Obtaining the correct value for the matrix element clearly is important whenever a golden rule formulation of the ET rate process is employed (since rate $\propto H_{\text{ab}}^2$).¹⁸ Even under so-called adiabatic dynamical conditions, however, the parameter is important because it helps to describe the shapes of the pertinent potential energy surfaces, particularly in the surface intersection region.¹⁹ Figure 3

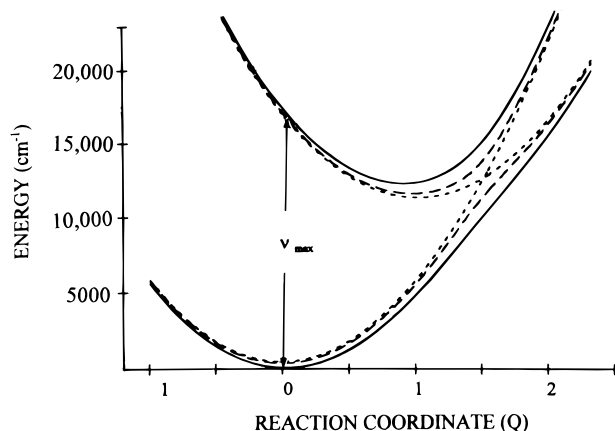


Figure 3. Potential energy surfaces for optical and thermal electron transfer in $(\text{NC})_5\text{FeCNOs}(\text{NH}_3)_5^-$. Dotted line: diabatic surfaces. Dashed line: adiabatic surfaces with $H_{ab} = 1260 \text{ cm}^{-1}$. Solid line: adiabatic surfaces with $H_{ab} = 2600 \text{ cm}^{-1}$.

illustrates how the diabatic potential energy surfaces for reaction 1 are modified when H_{ab} is employed as a first-order perturbation. Again, note the large correction that is introduced when the Stark-derived coupling parameter is used in place of the geometrically derived parameter. On the basis of the magnitude of the correction, one could even anticipate, for less exothermic reactions (Marcus normal region reactions), conversion from activated back-electron transfer to barrierless back-ET. Evaluation of less exothermic systems is currently in progress.

Acknowledgment. We acknowledge helpful discussions with Dr. Bruce Brunshwig and Dr. Marshall Newton regarding data analysis and Prof. Stephen Boxer concerning experiment implementation. We also thank Dr. Newton for a preprint of ref 6. We thank the U.S. Department of Energy, Office of Research, Division of Chemical Sciences (Grant No. DE-FG02-87ER13808) and the Dreyfus Foundation (Teacher-Scholar Award to J.T.H.) for support of this research.

References and Notes

- (1) (a) Oh, D. H.; Boxer, S. G. *J. Am. Chem. Soc.* **1989**, *111*, 1130. (b) Gottfried, D. S.; Steffan, M. A.; Boxer, S. G. *Biochim. Biophys. Acta*

1991, *1059*, 76. (c) Lao, K. Q.; Moore, L. J.; Zhou, H. L.; Boxer, S. G. *J. Phys. Chem.* **1995**, *99*, 496. (d) Boxer, S. G. In *The Photosynthetic Reaction Center*; Academic Press: New York, 1993; Vol. II, pp 179–220.

(2) (a) Oh, D. H.; Boxer, S. G. *J. Am. Chem. Soc.* **1990**, *112*, 8161. (b) Oh, D. H.; Sano, M.; Boxer, S. G. *J. Am. Chem. Soc.* **1991**, *113*, 6880.

(3) Shin, Y. K.; Brunshwig, B. S.; Creutz, C.; Sutin, N. *J. Am. Chem. Soc.* **1995**, *117*, 8668.

(4) Reimers, J. R.; Hush, N. S. *J. Phys. Chem.* **1991**, *95*, 9773.

(5) Creutz, C.; Newton, M. D.; Sutin, N. *J. Photochem. Photobiol. A: Chem.* **1994**, *82*, 47.

(6) Cave, R.; Newton, M. D. *Chem. Phys. Lett.* **1996**, *249*, 15.

(7) Hupp, J. T.; Dong, Y.; Blackburn, R. L.; Lu, H. *J. Phys. Chem.* **1993**, *97*, 3278.

(8) Burewicz, A.; Haim, A. *Inorg. Chem.* **1988**, *27*, 1611.

(9) Vogler, A.; Osman, A. H.; Kunkley, H. C. *Inorg. Chem.* **1987**, *26*, 2337.

(10) (a) Walker, G. C.; Barbara, P. F.; Doorn, S. K.; Dong, Y.; Hupp, J. T. *J. Phys. Chem.* **1991**, *95*, 5712. (b) Tominaga, K.; Klinner, D. A. V.; Johnson, A. E.; Levinger, N. E.; Barbara, P. F. *J. Chem. Phys.* **1993**, *98*, 1228. (c) Reid, P. J.; Silva, C.; Barbara, P. F.; Karki, L.; Hupp, J. T. *J. Phys. Chem.* **1995**, *99*, 2609.

(11) (a) Doorn, S. K.; Dyer, R. B.; Stoutland, P. O.; Woodruff, W. H. *J. Am. Chem. Soc.* **1993**, *115*, 6398. (b) Doorn, S. K.; Dyer, R. B.; Stoutland, P. O.; Woodruff, W. H. *J. Am. Chem. Soc.* **1992**, *114*, 3133.

(12) (a) Dong, Y.; Hupp, J. T. *Inorg. Chem.* **1992**, *31*, 3170. (b) Dong, Y.; Hupp, J. T. *Inorg. Chem.* **1992**, *31*, 3322. (c) Doorn, S. K.; Hupp, J. T. *J. Am. Chem. Soc.* **1989**, *111*, 1142.

(13) The power supply was based on the design used by both Boxer and co-workers^{1,2} and by Shin et al.³ and was constructed by Joseph Rolfe Associates of Palo Alto, CA.

(14) Liptay, W. In *Excited States*, Lim, E. C., Ed.; Academic Press: New York, 1974; Vol. 1, pp 129–229.

(15) F_{int} was estimated as 1.3 times the external field, based on the local field correction factor of 1.3 reported by Shin et al.³ for a similar matrix (1:1 glycerol:water).

(16) Karki, L.; Hupp, J. T.; Therien, M. J.; Lin, V. S. Y.; LeCours, S. M., manuscript in preparation.

(17) We assume that $\Delta\mu_{ab}$ is temperature independent. Equations 3–5 then yield $0.41 \text{ e} \cdot \text{\AA}$ for P_{12} and 2.5 \AA for R_{12} at 298 K, based on $\epsilon_{\text{max}}(298) = 3000 \text{ cm}^{-1} \text{ M}^{-1}$, $\Delta\nu_{1/2}(298) = 4400 \text{ cm}^{-1}$, and $\nu_{\text{max}}(298) = 16400 \text{ cm}^{-1}$.

(18) See: Brunshwig, B. S.; Ehrenson, S.; Sutin, N. *J. Phys. Chem.* **1986**, *90*, 3657. The mixed-valence chromophore was treated as an ellipsoid with a semimajor axis 12.4 \AA in length, a pair of semiminor axes 7 \AA in length and an interfolal distance of 10.2 \AA .

(19) For an erudite discussion, see: Sutin, N. *Prog. Inorg. Chem.* **1983**, *30*, 441.

JP9613551